IAEA nuclear fusion

PAPER • OPEN ACCESS

Final integration, commissioning and start of the Wendelstein 7-X stellarator operation

OPEN ACCESS
IOP Publishing | International Atomic Energy Agency Nuclear Fusion

Nucl. Fusion **57** (2017) 116015 (9pp) https://doi.org/10.1088/1741-4326/aa7cbb

Final integration, commissioning and start of the Wendelstein 7-X stellarator operation

H.-S. Bosch, R. Brakel, T. Braeuer, V. Bykov, P. van Eeten, J.-H. Feist, F. Füllenbach, M. Gasparotto, H. Grote, T. Klinger, H. Laqua, M. Nagel, D. Naujoks, M. Otte, K. Risse, T. Rummel, J. Schacht, A. Spring, T. Sunn Pedersen, R. Vilbrandt, L. Wegener, A. Werner, R.C. Wolf, J. Baldzuhn, C. Biedermann, H. Braune, R. Burhenn, M. Hirsch, U. Höfel, J. Knauer, P. Kornejew, S. Marsen, T. Stange, H. Trimino Mora and W7-X Team[a]

Max-Planck-Institut für Plasmaphysik, Greifswald, Germany

E-mail: bosch@ipp.mpg.de

Received 26 March 2017, revised 21 June 2017
Accepted for publication 30 June 2017
Published 3 August 2017

Abstract

The main objective of the Wendelstein 7-X (W7-X) stellarator is to demonstrate the integrated reactor potential of the optimized stellarator line. An important element of this mission is the achievement of high heating-power and high confinement in steady-state operation. Such an integrated plasma operation has not yet been demonstrated and represents the major scientific goal of W7-X. The way towards this goal is staged. In the first phase, called OP 1.1, December 2015-March 2016, a limiter configuration was used. In this paper, the preparation of the first operation phase as well as lessons learned during the first commissioning and the operation phase are discussed, while the physics results from OP 1.1 are reported elsewhere (Wolf *et al* 2017 *Nucl. Fusion* **57** 102020).

Keywords: operation, stellarator, Wendelstein 7-X

(Some figures may appear in colour only in the online journal)

1. Introduction

At the Max-Planck-Institute for Plasma Physics in Greifswald, the numerically optimized stellarator Wendelstein 7-X (W7-X) [2, 3] was constructed and assembled over the past years. The mission of this device is twofold: It has to demonstrate the stellarator optimization, but in the long term it also has to prove the steady-state capabilities of the stellarator concept. With a confining magnetic field independent of the plasma itself, i.e. generated predominantly by external coils only, plasma confinement is intrinsically steady-state. The main mission of W7-X is to demonstrate steady state operation in plasma regimes relevant for a fusion reactor. The way towards this steady-state operation, however, is staged. In the first operational phase, called OP 1.1, a limiter configuration was used for first plasma operation. With five graphite limiters at the inner wall, only a few graphite tiles on the inner side (opposite of the ECRH launchers) had been installed. As a result, the energy delivered into the plasma was restricted to 4 MJ. In this phase, from December 2015 until March 2016, first experience with the device itself, the control systems and the diagnostics was gained. The first commissioning, the transition to the operation phase OP 1.1 and the lessons learned, are the topics of this paper.

Presently, in the completion phase for OP 1.2, an inertially cooled test divertor with 10 modules (2 in each of the 5 modules of W7-X, one at the bottom and one on top of the plasma vessel), and a fully C-covered inner wall are installed. Therefore, the energy per plasma pulse during the second operational phase, OP 1.2, scheduled for 2017/18, will be

[a] See the author list of ‘Major results from the first plasma campaign of the Wendelstein 7-X stellarator’ by R. Wolf *et al* in the *Nuclear Fusion* Special issue: overview and summary reports from the *26th Fusion Energy Conference (Kyoto, Japan, 17–22 October 2016)*.

increased to 80 MJ. Only in the third operational phase (OP 2), an actively water-cooled divertor, water-cooled panels and wall tiles and cryo pumps will be installed, aiming at steady-state operation. For technical reasons this pulse duration had to fixed by the cooling infrastructure to 1800 s, but this already beyond all physical time-scales. This phase is scheduled to start in 2020, but real steady-state operation is a scientific and technological goal that will require some time for its establishment.

2. Assembly and the preparation of the commissioning

Assembly of the W7-X device started in earnest in 2005, when the first modular, non-planar coils were threaded onto the first plasma vessel half-module [4]. The first out of five modules, with ten non-planar coils and four planar coils threaded around the plasma vessel module and fixed to the segment of the central support was ready in August 2008. After the installation of the cryo supply lines and bus-bars (superconducting connections between coils and between coils and the current leads), this first module of the magnet system was placed in the lower shell of the cryostat vessel, already positioned on the machine base in the torus hall, end of October 2009, before the cryostat module was covered with the upper half. Then the access ports to the plasma vessel (about 51 per module, in total 254) were threaded and welded into the plasma vessel and the cryostat vessel. In November 2011 the fifth module was transferred onto the machine base and the cryostat vessel was closed shortly after that. After the port installation in this module and the assembly of the fourteen current leads [5] (for the seven electrical circuits for the superconducting coils, with 10 coils of one type connected in series), the cryostat (composed of plasma and cryostat vessels and the 254 ports between them) was closed in March 2014. At this time, the commissioning of W7-X was started. The installation of the in-vessel components, diagnostic systems and of peripheral components was continued (see figure 1). Different aspects of the assembly process are described in [6].

The assembly process which took about 1000 000 man-hours up to March 2014, was essentially dominated by the high demands on tolerances for the position of the superconducting coils [7]. For both reasons, high-precision manufacturing tools and extensive geometrical measurements have been applied during the manufacturing process of the main field coils. In the end, the as-built current path of the coils deviates only by some millimetres from their design geometry. The deviations between the as-built current paths of single coils of the same type show much less differences.

In each out of the five main assembly steps all magnet system components were aligned with a tolerance of 1.5 mm or less. In addition to the high alignment efforts, a numerical optimizing process was introduced taking into account all known geometrical data to improve the resulting magnetic field topology before the final alignment of all five magnet system modules. Finally, all 70 main field coils show an average alignment deviation of 1.2 mm, whereas the maximum deviation of any coil fiducial mark does not exceed 4.4 mm [8].

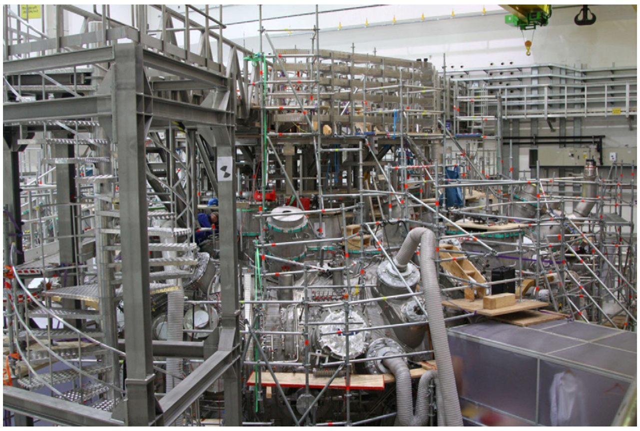

Figure 1. Wendelstein 7-X in March 2015. The last weld on the cryostat vessel is visible between the two domes in the middle of this picture. The hoses on the ports right of that are used for the air supply in the plasma vessel during the assembly of the in-vessel components. In the lower right corner one of the access booths is visible. On top of the device, cable trays can be seen.

The commissioning of W7-X was prepared carefully, based on the technological sequence [9], but also taking the formal processes and the corresponding quality assurance measures into account [10]. In advance of the commissioning, the behaviour of the device was simulated with finite element modelling (FEM) to confirm the structural integrity of the stellarator during design of the components and the device, all commissioning steps, but also to know where sensitive locations are present, to equip those with additional instrumentation [11] and to establish reference values, which during commissioning can be compared to the measurements. These analyses were performed for all relevant loads: temperature gradients, pressure, deadweight, induced displacements and/or electromagnetic forces.

3. Commissioning of W7-X

3.1. Cryostat

The integral commissioning started after the closure of the cryostat [12] with the startup of the interspace vacuum system, pumping the interspaces of the multilayer port bellows, the double sealed flanges at the outer vessel and on the plasma vessel as well as the combined water- and current feeding system for the control coils. In July 2014, the cryostat was pumped-down for the first time, and at the same time the mechanical integrity of the cryostat was confirmed. Movements and deformations of the outer vessel and the port bellows during this pump down agreed rather well with the corresponding FE modelling [13, 14], see figure 2 for a typical displacement plot.

3.2. Cryosupply

At the same time, the cryo-piping outside the cryostat was completed. After a check and the approval by the authorities, the cryo-system was commissioned locally. This lengthy procedure started in fall of 2014 with the leak-search and cleaning of the 2000 m of piping. The cleaning of the piping inside the cryostat was performed by sudden expansion of nitrogen gas.

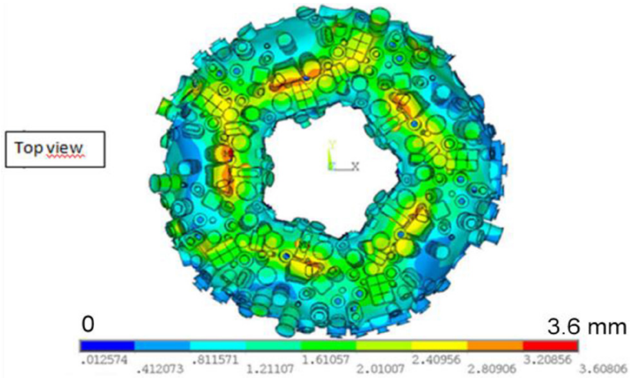

Figure 2. Deformations of the outer vessel shell, as calculated with a FE model for the load case of cryostat evacuation.

Subsequently, the piping was purged and filled with helium gas a few times before the helium was circulated in the full cryo system circuit and cleaned with the cold absorber system of the cryo plant. The cryo plant, which had been stopped after its commissioning beginning of 2013, was re-commissioned late in 2014. After the mentioned preparations had been finished, the in-vessel installations completed, the neutron detector calibration finished and the plasma vessel closed, the W7-X magnet system was cooled down together with the cryo plant, starting middle of February 2015.

After less than 4 weeks the superconducting coil set together with the mechanical support structure, i.e. a total mass of 430 tonnes, were cooled down successfully to 4 K without any problem [15], see figure 3. Subsequently different cryogenic operation modes were successfully commissioned, the standard mode at about 4 K for magnet operation up to 2.5 T, and the short standby mode at around 10 K for night and weekend breaks.

During this cooling down period no collisions between neighbouring components inside the very tight cryostat-vessel, e.g. bus bars and cryo-pipes were observed, although these components were shrinking and the magnet system sliding support moved by up to 11 mm [16]. These effects had also been calculated and taken into account in the design. However, the margins were rather small. Mechanical measurements during the cooling process confirmed the corresponding FE modelling.

3.3. Plasma vessel and non-superconducting coils

In parallel to this long phase of commissioning the cryo supply system, other components were taken into operation. During the commissioning of the plasma vacuum system, a systematic failure was found in the pump duct seals of all turbo molecular pumps. After replacement of 80 DN400 CF seals with an improved assembly technology, the pump down of the plasma vessel was successful. A plasma vessel pressure of $1 * 10^{-6}$ mbar was achieved with 12 turbo pumps (out of 30 available in total) after two weeks. During that time the initial leak rate of the plasma vessel could be decreased by repairing 13 leaks (mainly bolts to be tightened correctly). Before bake-out a final pressure of $7 * 10^{-7}$ mbar was achieved.

The plasma vessel is seated on 15 columns which carry the weight, but at the same time allow lateral movements of the plasma vessel due to its shrinking during cool-down. This mechanism is called the pendulum support. Figure 4 shows the evolution of the vertical loads between the three pendulums within one module due to the deformation of the plasma vessel during evacuation. The predicted load distribution as a function of the measured load corresponds very well to the AEA41 and the AFF40 pendulum support measurements. The AEX41 shows less reduction of the loads during the pump down than predicted. Since the AEX pendulums are close to the neighbouring plasma vessel module, the load distribution on this pendulum is very sensitive to the boundary conditions. An important check concerned the overall pendulum load staying constant over time. This was confirmed by measurements performed between April 2014 and July 2015.

In addition to the superconducting coils, W7-X also has two normally conducting coil systems (i.e. water-cooled copper coils) which were commissioned in parallel to the other tasks:

(a) Ten ’control coils‘ inside the plasma vessel, behind the divertor targets [17] to sweep the divertor strike point with up to 20 Ht over the target and to equalize the power load onto the 10 divertor targets. This system was commissioned in the time April-November 2015.
(b) In addition, five ‘trim coils’ are mounted on the outside of the cryostat (symmetrically to the midplane) [18]. These, independently supplied, coils can be used for physics studies related to the correction stellarator-symmetry-breaking magnetic errors. For this, each of the power supplies can provide the coil currents in both directions. This system has been commissioned in fall of 2014 [19].

3.4. Superconducting coil system

Following the cryo supply tests, the superconducting magnet system was taken into operation [20]. As the system consists of 70 coils with 7 types, always 10 coils of a type are connected in series and have an independent power supply. First each of these 7 circuits was tested individually up to current level of 5–12.8 kA (depending on coil type and mechanical limitations), including adjusting the quench detection (QD) detectors [21]. Figure 5 shows, as a typical example, current test at the 12.8 kA level for the non-planar coils of type 4. The test cycle has different current ramps (red line) including slow and fast discharges. Also shown is the He-temperature in the course of the circuit, starting with 3.9 K at the inlet, with the coil outlets at 4.05–4.5 K and ending at the current leads (4.6 m busbar after the last coil), where the helium leaves the cryostat with a temperature of about 5 K.

After commissioning of all the individual circuits, the whole system with 70 coils was successfully commissioned in a similar way. After integral commissioning of the magnet system, the vacuum magnetic flux surfaces were measured with an electron beam [22]. An electron beam (fixed at the end of a manipulator) is started inside the plasma vessel. The electrons follow the magnetic field lines and can be visualized

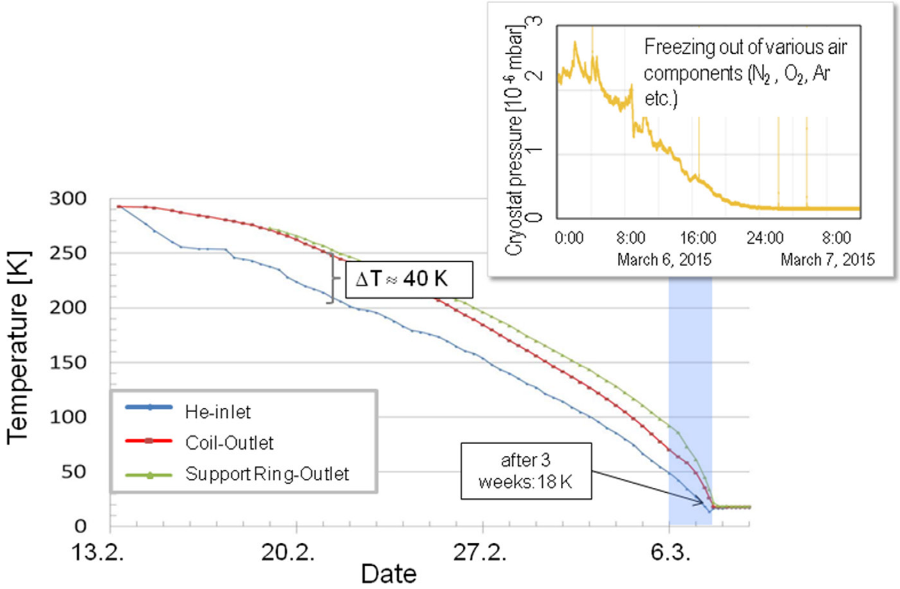

Figure 3. Cool-down of the W7-X magnet system in the first quarter of 2015. In less than 4 weeks, the magnet temperature reached 4 K. During the cool down, the He-temperature was controlled to keep the difference between He-inlet and outlet below 40 K in order to avoid too high mechanical stresses. Below a temperature of 10 K, see the gray bar and in the insert, various air component were frozen out, decreasing the cryostat pressure dramatically.

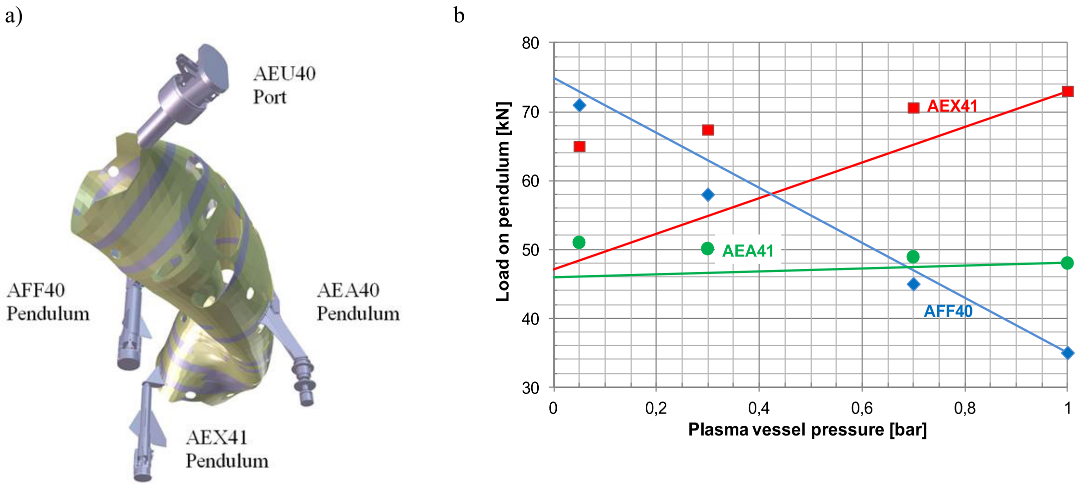

Figure 4. Pendulum support positions on single plasma vessel module (*a*) and the pendulum support loads (*b*) measured on module 4. The data points are the measured values, the predictions are shown as solid lines, more details on the calculations can be found in [14]. Reprinted from [14], Copyright 2017, with permission from Elsevier.

with a fluorescent stick, moved through the poloidal plane with a second manipulator. With this, a poloidal projection of a magnetic flux surface can be visualized and compared to the calculated magnetic flux surfaces. These results confirmed that the required tolerances, in all phases from the winding pack and coil fabrication to the assembly of the coils within a module and the general position of all modules, were successfully met [23].

3.5. Baking and preparation of operation

In August 2015, the plasma vessel was baked at 150 °C for 10 d with a plateau of 7 d [14]. This baking was performed with pressurized hot water in the plasma vessel and port cooling/heating pipes located outside the plasma vessel. The superconducting coils are protected by a thermal insulation on the cryostat walls and the cryostat vacuum; furthermore, they are kept at around 8–9 K by the liquid helium during the baking. The diagnostic ports, connecting the plasma vessel to the torus hall, were heated electrically to about 150 °C. After the baking and some leak repairs, a plasma vessel pressure of $2 * 10^{-8}$ mbar was achieved, as compared to $7 * 10^{-7}$ mbar before the baking.

The plasma vessel support system (figure 4) enables free expansion of the PV during baking. The FE Global Model of the Cryostat System predicts the expansion of the plasma vessel and ports assuming a uniform 150 °C temperature distribution on these components (figure 6). The radial displacement of the 5 horizontal AEU-Ports as measured by the so-called pyramids (figure 6, lower traces) is ~30% lower than the predicted displacement. This is most probably due to the non-uniform temperature of the PV and some cooler ports with temperatures only between 100 and 150 °C.

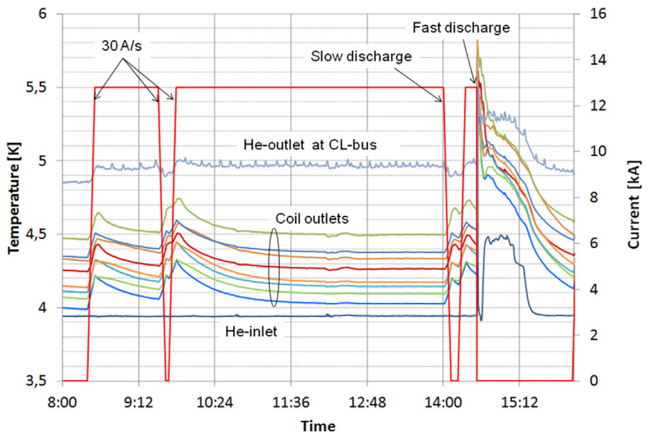

Figure 5. Current tests for the non-planar coils type 4. The coil current is shown in red (right scale), all other lines show the He-temperature (left scale). The cold He enters W7-X with a temperature of 3.9 K and is heated up while flowing though the coils and leaves W7-X with about 5.3 K at the current lead.

Subsequently the magnetic flux surface measurements were continued to further check the influence of the trim coils to alter the magnetic islands near the plasma surface. For these investigations specialized field configurations were used [24]. About 25 diagnostics systems were finalised and commissioned in the fall 2015 [25], as well as the ECRH-system which was commissioned with six gyrotrons, capable of delivering about 4.3 MW into the plasma with steerable antennas from the low field side of the plasma [1].

In parallel to preparing the hardware, also software packages had to be commissioned. The steady-state archiving of technical and experimental data was operational during the full period of commissioning, but the number of components was largely increased during this time [26].

The activities to get the operation permit from the authorities of Mecklenburg–Vorpommern were a major issue. The authorities ordered the German Association for Technical Inspections (TÜV Rheinland) to check the W7-X safety report and the necessary safety measures. The final assessment by the TÜV resulted in a few, rather late modifications of safety systems (radiation protection system, access system and the control system for keeping the torus hall free of persons). This also concerned the central safety system (cSS), which has been developed according to the standard IEC 61511. Following the safety analyses for all components, including heating and diagnostics systems, a risk analysis has been performed for all possible faults with regards to personnel safety and device safety (investment protection). For each of these risks, a safety instrumented functions (SIF) has been formulated and the respective safety integrity level (SIL) derived [27]. The hardware for the cSS is based on a fail-safe redundant Simatic S7-400 safety PLC (programmable logic controllers). The full cSS chain (sensor-logic-actor) has been developed and validated according to IEC 61511 and approved by the TÜV. For OP 1.1, the cSS included 27 SIFs for personnel safety and 9 SIFs for machine safety. Some of the risks were handled by organisational means only, i.e. by explicit actions from machine operators or by components ROs, as foreseen in the standard IEC 61511.

4. The first operation of W-X

In December 2015, the W7-X Segment Control system—the fast plasma control system—was commissioned [28, 29]. Because it has been built as a hierarchical distributed control system, all subsystems have already been tested during each component's commissioning. W7-X Segment Control is based on an arbitrary segmented program sequence description: It has been designed for fast synchronized steady-state control of both technical components (gas, heating …) and diagnostics and is capable of continuous data acquisition. Its flexibility allows executing dry runs or technical component tests using the same set-up and monitoring tools.

After the permit to operate W7-X was issued on December 9, the first helium-plasma was ignited on December 10, 2015. Operation started with helium for safety reasons. A short 20 ms helium gas puff via a-valve provided the gas target for ECRH, which was launched 100 ms after the gas puff by two gyrotrons with 500 kW each. Plasma break down was successfully achieved in the first attempt but ECRH absorption was lost after 10 ms, probably due to the influx of impurities originating from the plasma facing components.

4.1. Wall cleaning

By repeated application of ECRH conditioning cycles the gas load from the walls was reduced resulting in plasma phases extended to 50 ms. These cleaning sequences were provided by the Segment Control system which allowed to perform up to 20 consecutive short discharges within one experiment run. For this, discharge scenarios with up to 3 MW ECRH power, 50 ms pulse length and 30 s dwell time to allow for pumping between the pulses, have been programmed and repeated within one segmented program. The resulting experiment programs with more than 10 min length run successfully—proving the steady state capabilities of the W7-X Segment Control for long experiment phases as expected in future W7-X operation phases.

Further improvement was achieved with the availability of the glow discharge conditioning (GDC) system. The system consists of ten water-cooled disc shaped anodes which are integrated in the first wall, each being capable to be independently operated with a current up to 3 A. In OP1.1 seven anodes have been used with currents up to 1.2 A, providing an average current density to the wall up to 4 μA cm^{-2}. The discharges were operated in Helium. Ignition was achieved by voltages up to 3 kV at elevated He-pressure of $\approx 5 \times 10^{-2}$ mbar. After ignition the pressure was reduced to a level which was still compatible with stable burn (see figure 7). With improving wall conditions the burn pressure could be reduced down to 4×10^{-3} mbar.

After the first application of 15 min helium glow discharges, duration the ECRH absorption phase increased to about 100 ms, but degraded steadily in the following plasma discharges [30].

Plasma performance improved substantially with the operational time. Additionally, the length of GDC was extended up to 40 min, providing excellent conditions for the early

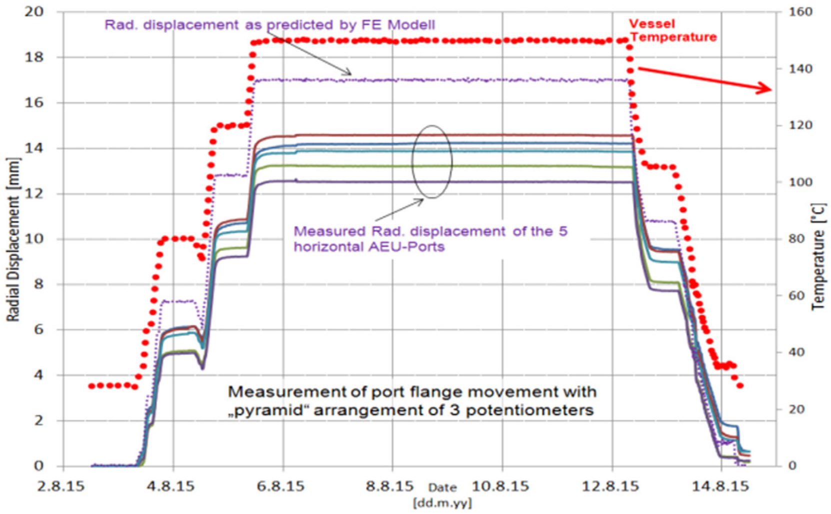

Figure 6. Radial displacement of AEU ports during baking.

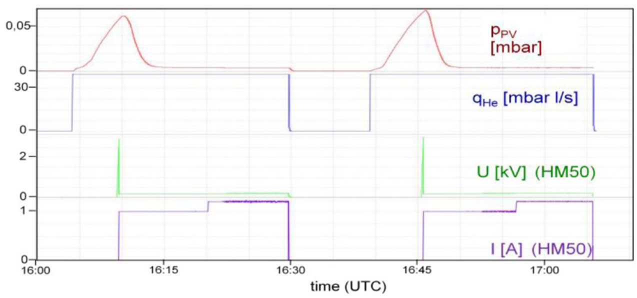

Figure 7. Helium glow discharge cycle with two 20 min burn phases, interrupted by a 15 min pumping phase. He-pressure and flow and voltage and current of one anode are shown.

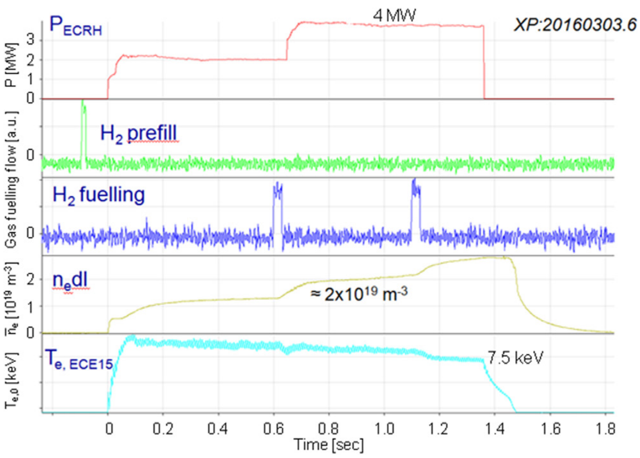

Figure 8. Hydrogen discharge with 2/4 MW ECRH power and increasing densities (Exp. 20160303.6). The electron temperature measurement shows a ECE channel at a position about 4 cm from the plasma centre. With controlled gas puffing the density could be adjusted to higher levels.

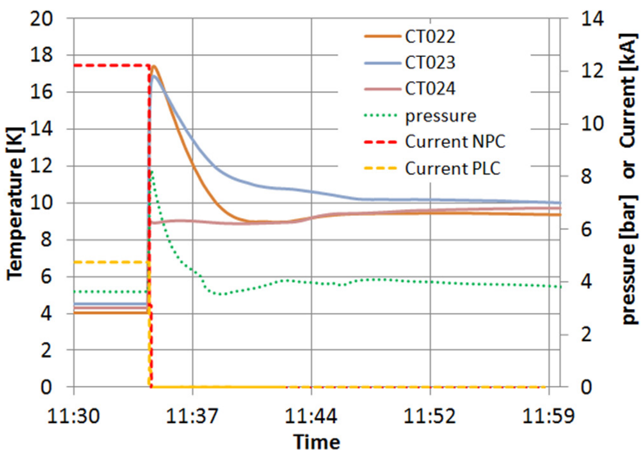

Figure 9. Temperature rise for three sensors (CT022, CT023, CT024) at the coil AAB44 casing during a fast shut down of the magnet system starting from 12.2 kA for the non-planar and 4.8 kA for the planar coils (solid line, scale is on the left axis). The current for the non-planar and planar coils are plotted as well (yellow and red broken line, scale on the right). In addition, the He pressure development in the conductor cooling is shown (dotted green line, scale on the right).

discharges of a day. ECRH conditioning with helium was rather effective to remove hydrogen from the walls.

During the first H-plasmas the ECRH-absorption phase reached 200 ms with 2 MW of heating power. However, the discharges were still limited by an uncontrollable density increase which provoked a radiation collapse. This improved rapidly with progressing plasma operation. Eventually, a pulse length of 6 s was possible at moderate heating power of 0.6 MW and constant line-averaged density of 7×10^{18} m^{-3}. Long discharges are of particular importance for W7-X, since the time scales for the development of internal plasma currents can be in the order of many seconds. Full density control was not achieved with the present limiter configuration even with hydrogen. The effective recycling coefficient was limited to $R_{\mathrm{eff}} = 1$, i.e. without external gas fuelling the density stayed constant. However, with controlled gas puffing the density could be adjusted to higher levels, see figure 8. With the future divertor configurations and less gas reservoirs in the walls, the situation is expected to improve.

4.2. Magnet operation

During the first operational phase of W7-X the superconducting magnet system provided a magnetic field of 2.5 T at the area where the ECRH waves should be absorbed by

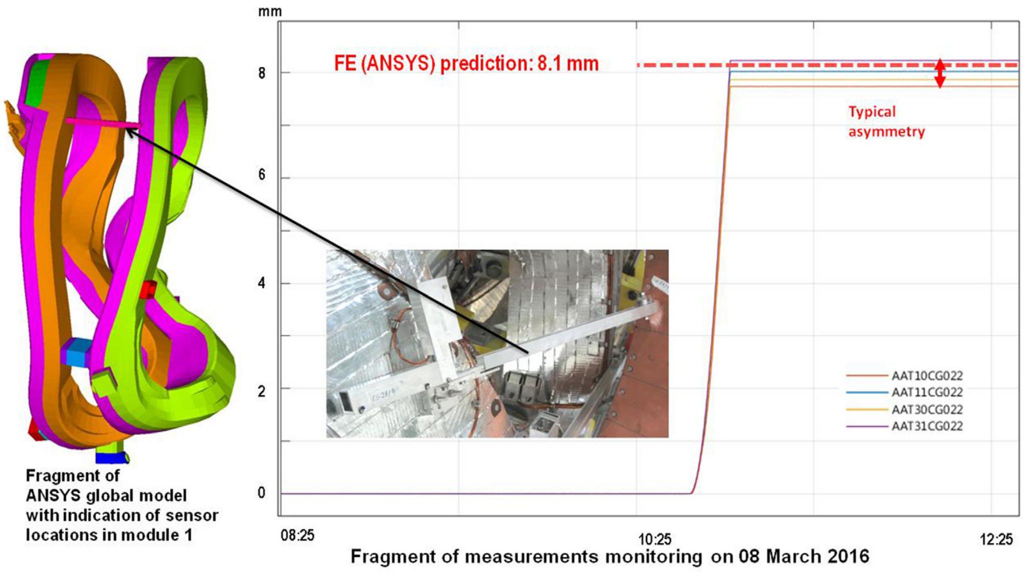

Figure 10. Comparison of numerical prediction for maximum measured displacement between non-planar coils with monitoring results during operation.

the plasma [31, 32]. The magnet system was operated with the magnetic field configuration 'OP1.1 Limiter' which was defined with 12.8 kA in the five non-planar coil circuits and 5 kA in the two planar coil circuits respectively. To shift the ECRH resonance closer to the plasma centre, the coil currents were fine tuned in small steps. The configuration with 12.37 kA in the non-planar circuits and 4.82 kA in the planar coil circuits was found to be the optimum regarding the absorption of the ECRH waves.

Parallel to the superconducting coils, the 5 normally conducting trim coils was operated during OP1.1 several times. The trim coils allow a fine tuning of the main magnetic field and work as a tool to influence field errors disturbing the toroidal periodicity.

The superconducting magnets were energized 35 times up to 2.5 T level during OP1.1, for a total of about 183 h spread over 31 operation days. The stored energy in the superconducting magnets at 2.5 T reached a level of 430 MJ. The availability of the magnet system was approximately 94%. During the OP1.1 phase no quench occurred, because the safety margin of 1 K could be kept all the time. One fast discharge of the superconducting magnet system was triggered due to a rapid discharge of the normally conducting trim coil system which influenced the QD system, see next chapter.

4.3. Cryogenic supply system

The cooling of the cryogenic system is achieved with a helium cryo plant with a nominal cooling power of 7 kW at 4.2 K. The specified mass flow rates and inlet temperatures for the different cooling circuits could be achieved for the standard mode used for the plasma operation. Coil conductors and coil casings were cooled with supercritical helium at 3.9 K and a mass flow rate of 500 g s^{-1}. The heat load on the coils and on the cold support structure was 682 W. The average helium outlet temperature at the coils is 4.2 K. When the non-planar coils are operated at 12.8 K, the outlet temperature rises by 0.05 K only in the steady state condition. The individual currents leads using high temperature superconducting tapes were cooled with helium gas at 50 K and a flow rate of 0.94 g s^{-1}. The load on the actively cooled thermal shield was in the range of 6 W m^{-2} and sums up to 5.6 kW [15].

Table 1. Statistics of the experiments in OP 1.1. Especially the cleaning experiments often used up to 20 plasma pulses in one experiment.

Experiment type	Experiments	Plasma pulses
Plasma discharges	631	640
Cleaning pulses with ECRH	145	1282
Test pulses	148	148
Fault pulses	24	24
	948	2094

During a rapid shut down of the magnet system the current is reduced with a time constant of about 2–3 s. Such an event was triggered on the 25th of February 2016 with a current of 12.2 kA in the 50 non-planar and 4.8 kA in the 10 planar coils. Eddy currents were induced in the coil conductor and in the coil casing leading to a warm up of the coil casings and consequently to heating of the helium (see also in figure 5, after the fast discharge). Therefore the heated helium was expulsed from the coils. The pressure in the He- manifolds inside the cryostat rose up to 8.0 bars, which resulted finally in a shutdown of the whole cryo plant. Figure 9 shows the temperature rise at three locations on the casing of non-planar coil type 4 (AAB44). The temperature sensors CT022 and CT023 rose from 4 K to about 17 K. The third sensor (CT024) rose only to 9 K. Within half an hour, the casing temperatures equalized at 10 K. After such an event, several hours are required to get back to a normal operation condition.

The cryogenic system was operated continuously for about 14 months. During that period the cryo plant operated quite reliable. Altogether seven trips of the whole cryo plant occurred that were caused either by components of the plant itself (e.g. valves and instrumentation) or by external supply systems (water and electrical supply). Nevertheless a restart of the cryo plant was possible within several hours up to 2 d in one case.

4.4. Mechanical behaviour of the superconducting coils

The strong backing through numerical modelling and mechanical instrumentation monitoring strongly supported and certified the structural integrity of W7-X main systems [33] during OP 1.1. Figure 10 shows comparison between FE prediction and maximum measured displacement between non-planar coils in four different half-modules. All four measurements lie in the same area with only small deviations among each other and in the tolerance band of the FE modelling.

4.5. Operation summary

To perform the physics experiments in W7-X, the Control and Data Acquisition group provided an integrated framework to configure, control and monitor physics experiments [28]. Up to the end of the operation phase OP 1.1, on March 10, 2016, 948 experiments were run, i.e. 776 plasma experiments, as listed in table 1. Due to the sequences of multiple plasma pulses in one experiment run, the number of plasma pulses was much higher, adding up to 2094 plasma pulses. 148 technical experiments were used for commissioning and improvements of timing systems, diagnostics and ECRH, 24 experiments were considered as faulty.

Measurement and pre-analyzed data from 59 integrated data sources, both technical components and diagnostics, have been streamed continuously to the W7-X archive—reliably since more than two years. Besides data streaming from fully integrated systems, data have been uploaded between experiment runs from more than 100 external sources as well as from data analyses, adding up to 10 TB of data in March 2016 (25 TB as for today).

5. Conclusion

After a detailed commissioning process, which took advantage of the detailed FEM modelling of the W7-X device, and carefully comparing the measurements (mechanical as well as electrical and thermo-dynamical) with these predictions, Wendelstein 7-X was commissioned successfully in December 2015. During the operation phase OP 1.1, which was concluded in March 2016, about 950 experiments were run, more than 66 % of them investigating physics question [1].

Acknowledgment

This work has been carried out within the framework of the EUROfusion Consortium and has received funding from the Euratom research and training programme 2014–2018 under grant agreement No 633053. The views and opinions expressed herein do not necessarily reflect those of the European Commission.

ORCID iDs

H.-S. Bosch https://orcid.org/0000-0003-0621-6913

References

[1] Wolf R. *et al* 2017 Major results from the first plasma campaign of the Wendelstein 7-X stellarator *Nucl. Fusion* **57** 102020
[2] Grieger G. *et al* 1992 Physics optimization of stellarators *Phys. Fluids* B **4** 2018–91
[3] Nührenberg J. *et al* 1995 Overview on Wendelstein 7-X theory *Trans. Fusion Technol.* **27** 71
[4] Wegener L. *et al* 2005 Wendelstein 7-X at the transition to assembly *Fusion Eng. Des.* **74** 42–8
[5] Rummel T. *et al* 2014 The current leads of the Wendelstein 7-X superconducting magnet system *IEEE Trans. Plasma Sci.* **42** 2146–53
[6] Wegener L. *et al* 2009 Status of Wendelstein 7-X construction *Fusion Eng. Des.* **84** 106–2
[7] Bosch H.-S. *et al* 2013 Technical challenges in the construction of the steady-state stellarator Wendelstein 7-X *Nucl. Fusion* **53** 126001
[8] Braeuer T. *et al* 2013 Interaction of metrology and assembly at W7-X *Fusion Eng. Des.* **88** 721–7
[9] Gasparotto M. *et al* 2014 Wendelstein 7-X—Status of the project and commissioning planning *Fusion Eng. Des.* **89** 2121–7
[10] Vilbrandt R. *et al* 2015 Continuity and enhancement of quality management during commissioning of W7-X *Fusion Eng. Des.* **96–7** 337–77
[11] Bykov V. *et al* 2015 Wendelstein 7-X mechanical instrumentation system for commissioning and operation *Fusion Sci. Technol.* **68** 267–71
[12] Bosch H.-S. *et al* 2015 Experience with the commissioning of the superconducting stellarator Wendelstein 7-X *Fusion Eng. Des.* **96–7** 22–7
[13] van Eeten P. *et al* 2015 Features and analyses of W7-X cryostat system FE model *Fusion Eng. Des.* **96–7** 369–72
[14] van Eeten P. *et al* 2017 Monitoring of W7-X cryostat commissioning with cryostat system FE model *Fusion Eng. Des.* (https://doi.org/10.1016/j.fusengdes.2017.05.061)
[15] Nagel M. *et al* 2017 Cryogenic commissioning, cool down and first magnet operation of Wendelstein 7-X *IOP Conf. Ser.: Mater. Sci. Eng.* **171** 012050
[16] Bykov V. *et al* 2016 Structural analysis at the transition from W7-X construction to operation *IEEE Trans. Plasma Sci.* **44** 1722–30
[17] Stadler R. *et al* 2009 The in-vessel components of the experiment Wendelstein 7-X *Fusion Eng. Des.* **84** 305–8
[18] Rummel T. *et al* 2012 The trim coils for the Wendelstein 7-X magnet system *IEEE Trans. Appl. Supercond.* **22** 4201704
[19] Füllenbach F. *et al* 2017 The Wendelstein 7-X trim coil sytem commissioning and first operational results *Fusion Eng. Des.* (https://doi.org/10.1016/j.fusengdes.2017.03.104)
[20] Risse K. *et al* 2016 Wendelstein 7-X—commissioning of the superconducting magnet system *IEEE Trans. Appl. Supercond.* **26** 4202004
[21] Birus D. *et al* 2011 The quench detection system of Wendelstein 7-X *Fusion Eng. Design* **88** 1566–70
[22] Otte M. *et al* 2016 Setup and initial results from the magnetic flux surface diagnostics at Wendelstein 7-X, Plasma *Phys. Control. Fusion* **58** 064003
[23] Sunn Pedersen T. *et al* 2016 Confirmation of the topology of the Wendelstein 7-X magnetic field to better than 1:100 000 *Nat. Commun.* **7** 13493

[24] Lazerson S. *et al* 2016 First measurements of error fields on W7-X using flux surface mapping *Nucl. Fusion* **56** 106005
[25] Krychowiak M. *et al* 2016 Overview of diagnostic performance and results for the first operation phase in Wendelstein 7-X *Rev. Sci. Instrum.* **87** 11D304
[26] Henning C. *et al* 2016 ArchiveDB—scientific and technical data archive for W7-X *Fusion Eng. Des.* **112** 984–90
[27] Vilbrandt R. *et al* 2017 Application of the engineering standard for functional safety to the W7-X central safety system *Fusion Eng. Des.* (https://doi.org/10.1016/j.fusengdes.2017.02.066)
[28] Spring A. *et al* 2017 Establishing the Wendelstein 7-X steady state plasma control and data acquisition system during the first operation phase *Fusion Eng. Des.* (https://doi.org/10.1016/j.fusengdes.2017.03.127)
[29] Laqua H. *et al* 2017 Experiences with the segment control system at Wendelstein 7-X operation *Fusion Eng. Des.* (https://doi.org/10.1016/j.fusengdes.2017.03.066)
[30] Wauters T. *et al* 2016 Wall conditioning by ECRH and GDC at the Wendelstein 7-X stellarator *43rd EPS Conf. on Plasma Physics (Leuven, Belgium 2016)* P4.047
[31] Risse K. *et al* 2017 First operational phase of the superconducting magnet system of Wendelstein 7-X *Fusion Eng. Des.* (https://doi.org/10.1016/j.fusengdes.2017.03.050)
[32] Rummel T. *et al* 2017 Commissioning results of the superconducting magnet system of Wendelstein 7-X *IEEE Trans. Appl. Supercond.* **27** 1–7
[33] Bykov V. *et al* 2017 Engineering challenges of W7-X: improvement of numerical modelling and mechanical monitoring after commissioning and first phase of operation *Fusion Sci. Technol.* submitted